Performance improvement of a PEMFC system controlling the cathode outlet air flow

Diego Feroldi (corresponding author), Maria Serra, Jordi Riera

Institut de Robòtica i Informàtica Industrial

Universitat Politècnica de Catalunya - Consejo Superior de Investigaciones Científicas

C. Llorens i Artigas 4, 08028 Barcelona, Spain

E-mail: dferoldi@iri.upc.edu

Telephone: 34 93 4015805; fax: 34 93 4015750

ABSTRACT

This paper presents a stationary and dynamic study of the advantages of using a regulating valve for the cathode outlet flow in combination with the compressor motor voltage as manipulated variables in a fuel cell system. At a given load current, the cathode input and output flowrate determine the cathode pressure and stoichiometry, and consequently determine the oxygen partial pressure, the generated voltage and the compressor power consumption. In order to maintain a high efficiency during operation, the cathode output regulating valve has to be adjusted to the operating conditions, specially marked by the current drawn from the stack. Besides, the appropriate valve manipulation produces an improvement in the transient response of the system. The influence of this input variable is exploited by implementing a predictive control strategy based on Dynamic Matrix Control (DMC), using the compressor voltage and the cathode output regulating valve as manipulated variables. The objectives of this control strategy are to regulate both the fuel cell voltage and oxygen excess ratio in the cathode, and thus, to improve the system performance. All the simulation results have been obtained using the MATLAB-Simulink environment.

Keywords: PEMFC, Multivariable Control, Predictive Control, Dynamic Matrix Control, Performance improvement

1. INTRODUCTION

Polymer Electrolyte Membrane (PEM) fuel cell systems are efficient devices which allow the transformation of chemical energy stored in hydrogen to electric energy. In order to obtain this transformation efficiently the global system, which includes several subsystems, must be considered. The air supply is one of these subsystems, which has a great influence in the system efficiency. At the same time, one of the most important challenges in fuel cell control is to assure sufficient amount of oxygen in the cathode when current is drawn abruptly from the fuel cell stack. In this study the air supply subsystem is composed by an air compressor, while the fuel supply subsystem relies on a pressurized hydrogen tank. The hydrogen inlet flow rate is regulated by an independent control loop to maintain the working pressure in the anode close to the pressure in the cathode. A schematic diagram of the system is showed in Fig. 1.

The PEM fuel cell system without a proper controller will not be able to withstand the load fluctuations [1]. When an electric load is connected to the fuel cell, the control system must maintain the optimal temperature, the membrane hydration and the partial pressure of the gases at both sides of the membrane in order to avoid voltage degradation and fuel cell life shortening [2]. In particular, the air supply results critical in the system performance because the oxygen reacts instantly as current is drawn, whereas the oxygen supply is limited by the dynamics of the inlet manifold and the air compressor [3]. The operating air pressure and the air stoichiometric ratio provided to the stack by the air supply subsystem, control the oxygen partial pressure at the cathode catalyst layer. This partial pressure has major influence in the cathode polarization and thus, in the conversion efficiency [4].

In several publications the control of air supply has been approached. In [5] is demonstrated the convenience of regulating the oxygen excess ratio in the cathode to maximize the system net power. The oxygen excess ratio or stoichiometric ratio is defined as the ratio of inlet oxygen flow to reacted oxygen flow in the cathode. In [2], [5], [6] and [7], the control of oxygen excess ratio is approached through the manipulation of the compressor motor voltage. In [2] and [5] feedforward control is employed, meanwhile in [6] and [7] model based predictive control (MPC) is employed. These works indicate that there is a severe conflict between oxygen excess control and net power dynamic response if no extra power source is employed. This limitation arises from the fact that all the power required by the air supply compressor comes from the fuel cell stack. In [6] supercapacitors are included as an ancillary power source in order to support the power peaks.

The voltage applied to the compressor motor is a suitable manipulated variable in order to control the oxygen excess ratio in the cathode, as it is showed in [2], [5], [6] and [7]. In this paper we propose to use a regulating valve for the cathode outlet flow in combination with the compressor motor voltage as manipulated variables to control both the oxygen excess ratio and the stack voltage. In [2], [5], [6] and [7], the stack output voltage is let unregulated. However, depending on the application, the regulation of the stack output voltage would be required.

The paper is organized as follows: In Section 2 a description of the fuel cell system model employed is done. Stationary and transient analyses of system performance are done in Sections 3 and 4, respectively. In Section 5, a control strategy based on predictive control is proposed. The results are presented in Section 6 and, finally, conclusions are stated in Section 7.

2. PEM FUEL CELL SYSTEM MODEL DESCRIPTION

This work utilizes the PEM fuel cell model proposed by Pukrushpan et al. [2]. This nonlinear model is used to represent the transient behaviour of the plant in the simulation analysis. The control oriented model for automation applications includes the transient phenomenon of the compressor, the manifold filling dynamics (both anode and cathode), reactant partial pressures, and membrane humidity. The stack voltage predicted by the model depends on load current, partial pressure of hydrogen and oxygen, fuel cell temperature and the contents of water in the membrane. Spatial variations are not included and constant properties are assumed in all volumes. Only temporary variations are present. The model also assumes that the inlet reactant flows in the cathode and in the anode can be humidified, heated and cooled rapidly. With respect to the considered dynamics, the model neglects the fast dynamics of the electrochemical reactions (time constant of 10^{-19} s). Temperature is treated as a constant parameter because its slow behaviour (time constant of 10^{2} s), allowing to be regulated by its own (slower) controller. The model represents a 75 kW fuel cell system with 381cells. For more model details see [2].

3. STATIONARY ANALYSIS

As it has been mentioned, the air supply subsystem has a strong influence in fuel cell performance. On the one hand, an insufficient air supply may cause oxygen starvation in the cathode, which causes voltage reduction and membrane life shortening. On the other hand, the compressor operation implies a power consumption that diminishes the system efficiency. The system efficiency is defined as [8]:

$$\eta_{sys} = \frac{V_{FC}}{1.482}\frac{(P_{FC} - P_{aux})}{P_{FC}} \qquad (1)$$

where the constant 1.482 results of using the higher heating value of hydrogen (ΔH=286kJmol^{-1}), V_{FC} is the fuel cell voltage, P_{FC} is the fuel cell generated power and P_{aux} is the power consumed by the auxiliary equipment. The compressor power represents the major consumption in the auxiliary subsystem and is the only parasitic power considered in this work.

The operation at a higher pressure increments the generated voltage as a result of the increment in the cathode oxygen partial pressure and anode hydrogen partial pressure:

$$E = 1.229 - 0.85\times10^{-3}(T_{FC} - 298.15) + 4.3085\times10^{-5}T_{FC}\left[\ln(p_{H_2}) + 0.5\ln(p_{O_2})\right] \qquad (2)$$

where E is the generated voltage in a single cell in open circuit in volts, T_{FC} is the fuel cell temperature in Kelvin, p_{H2} and p_{O2} are the cathode partial pressure of hydrogen and oxygen, respectively, in atm. Nevertheless, an increment in the operating pressure implies a higher consumption of power in the air compressor, contributing to a reduction in the system efficiency. In fact, an increment in the cathode pressure produces an increment in the supply manifold pressure and thus, an increment in the pressure ratio across the compressor and in the compressor power consumption. The power consumed by the air compressor is:

$$P_{CM} = \frac{C_p T_{atm}}{\eta_{CP}}\left[\left(\frac{p_{sm}}{p_{atm}}\right)^{\frac{\gamma-1}{\gamma}} - 1\right]W_{CP} \qquad (3)$$

where W_{CP} is the compressor air flow rate, P_{CM} is the compressor power, T_{atm} is the inlet air temperature in the compressor, η_{CP} is the compressor efficiency, p_{sm} is the supply manifold pressure, C_p is the specific heat capacity of air, equal to 1004 J·kg^{-1}·K^{-1} and γ is the ratio of the specific heats of air equal to 1.4.

The compressor motor voltage as a control input allows regulating the oxygen partial pressure in the cathode. Augmenting the compressor voltage the oxygen partial pressure increases. However, the compressor power consumption also increases. Thus, it is important to employ a complementary way to increment the oxygen partial pressure. A diminution of the area of the valve that closes the cathode air flow contributes to increase the cathode pressure and at the same time, contributes to decrease the air flow, the stoichiometry, and the oxygen concentration. The consumption of the compressor has two opposite trends: the trend to increase due to the pressure rise and the trend to decrease due to the flow reduction. When all these effects are taken into account, there is a positive balance in the total efficiency diminishing the valve area as we can observe analyzing the polarization (Fig. 2), efficiency (Fig. 3),

power compressor consumption (Fig. 4) and oxygen partial pressure curves (Fig. 5) plotted for two different valve areas and a certain compressor voltage (V_{cm} = 140V). It is important to note that the increase in the efficiency is not for all current densities. When the current density is high the flow and concentration reduction have a greater influence than the pressure increase and the result is a decrease in the oxygen partial pressure. In effect, the oxygen consumption is higher at higher current densities:

$$W_{O_2,rct} = \frac{M_{O_2} n A}{4F} i \qquad (4)$$

where $W_{O2,rct}$ is the rate of oxygen reacted, M_{O2} is the molar mass of oxygen equal to 32 x 10^{-3} kg mol^{-1}, n is the cell's number, A is the active cell area equal to 381 cm^2, F is Faraday number equal to 96485 C and i is the current density. Hence, the oxygen molar fraction in the cathode will be lower because of the oxygen starvation.

Depending on the operating pressure, the increment in efficiency happens along different current density ranges. With low operating pressures (lower compressor voltage, V_{cm}) the system efficiency increment due to the valve closure occurs only at low current densities, whereas with higher operating pressures (higher compressor voltage) the increment in system efficiency occurs along greater current densities ranges. This can be seen in Fig. 6 to Fig. 8. For V_{cm} = 100V the efficiency increment occurs only for current densities below 0.34 $A \cdot cm^{-2}$ (Fig. 6), for V_{cm} = 140V the increment occurs for current densities below 0.67 $A \cdot cm^{-2}$ (Fig. 3), while for V_{cm} = 180V the increment occurs for al the current densities analysed (Fig. 7). As can be seen in Fig. 8 for V_{cm} = 180V, the oxygen partial pressure rise, as a result of diminishing the valve area, occurs at all current densities. In Fig. 9, it can be seen how the efficiency changes with A_t for values between 20 to 40 cm^2.

As a conclusion of this stationary analysis, it can be stated that the cathode output valve area as well as the compressor motor voltage have to be adjusted in order to have high efficiency.

4. TRANSIENT ANALYSIS

Besides the possible performance improvement observed in the stationary analysis there is also an improvement in the transient behaviour using the cathode air flow valve as a manipulated variable. A preliminary transient analysis is made employing a DMC control strategy (the details of this control strategy are explained in the next section). The controlled variable in this analysis is the stack voltage. A stack current disturbance from 200A to 210A is applied to the fuel cell system in order to compare the disturbance rejection capability of the system. A comparison between the transient responses obtained

using only the compressor voltage as a control variable and the one obtained by using the opening valve area in combination with the compressor voltage is showed in Fig 10. The later shows a better behaviour with a reduction in the stack voltage time response from 0.6s to 0.4s.

5. CONTROL STRATEGY

The advantages of using the opening valve area together with the compressor voltage are exploited implementing a control strategy. This control strategy is based in Dynamic Matrix Predictive Control (DMC) and has two control objectives: *i)* to regulate the oxygen excess ratio in the cathode, λ_{O2}, and *ii)* the generated voltage, V_{FC}. As we explained before, the control of λ_{O2} is an indirect way to control the system efficiency [5]. The load current, I_{FC}, is considered as a disturbance to the fuel cell system. The compressor motor voltage by itself is not able to control both control objectives. Nevertheless, with the addition of the opening valve area control variable, A_t, this problem is solved. Therefore, the manipulated variables are: $u_1 = V_{cm}$ and $u_2 = A_t$.

The DMC uses the step response to model the process, taking into account only the p first samples until the response tends to a constant value, assuming therefore that the process is asymptotically stable. Thus, the predicted output can be expressed as:

$$\hat{y} = Gu + f \qquad (5)$$

where:

$$G = \begin{pmatrix} g_1 & 0 & \cdots & 0 \\ g_2 & g_1 & \cdots & 0 \\ \vdots & \vdots & \ddots & \vdots \\ g_m & g_{m-1} & \cdots & g_1 \\ \vdots & \vdots & \ddots & \vdots \\ g_p & g_{p-1} & \cdots & g_{p-m+1} \end{pmatrix} \qquad (6)$$

is the dynamic matrix constructed from the coefficients g_i obtained from the step response with prediction horizon p and control horizon m, u is the future control vector and f is free response, that means, the response that not depends of future control movements [9].

The DMC controller objective is to minimize the difference between the consignees, $w(t)$, and the process outputs in a least square sense with the possibility of including a penalty term on the control signal:

$$J = \sum_{j=1}^{p} R\left[\hat{y}(t+j \mid t) - w(t+j)\right]^2 + \sum_{j=1}^{m} Q\left[\Delta u(t+j-1)\right]^2 \qquad (7)$$

where *R* and *Q* are diagonal weight matrixes. With the matrix *R* it is possible to compensate the different ranges of values in the process outputs, meanwhile the matrix *Q* allows to give different weights to the control signals.

If there are no restrictions in the manipulated variables, the minimization of the cost function J can be realized making its derivative equal to zero, resulting:

$$U = (G^T RG+Q)^{-1} G^T R(w-f) \qquad (8)$$

Such as all the predictive control strategies, only the first element in the control vector calculated is sent to the plant. In the next iteration the sequence of control is calculated again using actualized information from the plant. The theoretical bases of the method are given in detail in [9].

There is a great interaction between the manipulated variables and the controlled variables, which makes difficult the realization of a decentralized control of the system [10]. The DMC resolves efficiently the interaction problem between manipulated variables and controlled variables. The multivariable controller implemented employs in his control algorithm an extended dynamic matrix that takes into account the interactions:

$$G = \begin{pmatrix} G_{11} & G_{12} \\ G_{21} & G_{22} \end{pmatrix} \qquad (9)$$

where each matrix G_{ij} contains the coefficients of the *i-th* step response corresponding to the *j-th* input. The matrix R and Q have now the following form:

$$R = \begin{pmatrix} R_1 & 0 \\ 0 & R_2 \end{pmatrix}; \quad Q = \begin{pmatrix} Q_1 & 0 \\ 0 & Q_2 \end{pmatrix} \qquad (10)$$

where R_i and Q_i are diagonal matrixes of dimension *p x p* and *m x m* respectively. Thus, a centralized multivariable controller it is proposed, which take into account the interactions between manipulated and controlled variables.

6. RESULTS

The control horizon *m*, the prediction control *p*, and the matrixes *R* and *Q* were adjusted, in the control algorithm, to achieve an adequate dynamic behaviour of the fuel cell system. The values of *R* and *Q* have a strong influence on the transient response obtained. This is especially true for the weight matrix *Q,* which reduces the control effort. The higher are the values in *Q*, the lower is the control effort, but the

response time is greater. The values chosen of Q and R are: Q_1 = diag(1,1,…,1), Q_2 =diag(0.5,0.5,…,0.5), R_1 = diag (5,5,…,5), R_2=(1,1,…,1). The values of m and p are 100 and 15, respectively.

The internal model utilized by the DMC controller has been obtained through the linearization of the nonlinear model described in Section 2 around the operating point corresponding V_{cm} = 187.5V, A_t = 20 cm^2, I_{st} = 190A, which gives a net power of 40 kW.

The simulation results of the controlled system with variations in the load current are presented in Fig. 12 to Fig 15. In Fig. 11 the perturbation profile is showed. Fig. 12 and Fig. 13 show the controlled variables (λ_{O2} and V_{FC}), while Fig. 14 and Fig. 15 show the manipulated variables (V_{cm} and A_t). As can be observed in the figures, the implemented controller has a good disturbance rejection: the stack voltage response has a peak (3.5% of V_{FC} variation for 15% of I_{FC} variation) that disappears in less than 0.5s, and the oxygen excess ratio response presents a peak (30% of λ_{O2} variation for the same I_{FC} variation) that vanishes in less than 1s.

The controller performance can be improved if the disturbance is measured and a step disturbance model is included in the control model used to predict the plant outputs. Comparisons between measured and non-measured disturbance approaches have been made. In Fig. 16 and Fig. 17 details of voltage stack and oxygen excess ratio responses are showed, respectively. The results obtained show a substantial improvement in the generated voltage response. The oxygen excess ratio response could be changed by adjusting the values of the weight matrixes.

The control algorithm implements a compensation mechanism to rectify the inevitable model errors and deal with non-measured disturbances. This compensation mechanism utilizes output values, and thus, assures zero error at steady-state.

The simulation analysis shows a good performance in a wide operating range around the linearization point despite the internal controller model is linear.

7. CONCLUSIONS

High efficiency level, long life cycle and good transient behaviour are fundamental issues for the success of fuel cell systems in energy and automotive market. Through a steady-state analysis it is showed that the system efficiency, in most of the current density range, can be improved by manipulating the cathode outlet air flow valve. The dynamic analysis performed also shows a transient response improvement with this additional manipulated variable. Taking advantage of these facts, this article proposes a control

strategy based on predictive control (DMC) that uses the compressor motor voltage together with the cathode air flow valve area as manipulated variables. The controlled variables are the stack voltage and the oxygen excess ratio. To predict the future process response, the control strategy makes use of a process model that is easily obtainable through step response. The simulation analysis shows an appropriate dynamic response, which can still be improved with the inclusion of the disturbance model. The control objectives have been accomplished with reduced control effort. This effort can be further reduced modifying the values of the matrix *Q*. This is particularly important because of practical limitations in the manipulated variables.

Acknowledgments

This work has been funded partially by the project CICYT DPI2004-06871-C02-01 of the Spanish Government, and the support of the Department of Universities, Investigation and Society of Information of the Generalitat de Catalunya.

NOMENCLATURE

A	fuel cell active area (cm^2)
A_t	cathode output valve area (cm^2)
C_p	specific heat capacity of air (1004 $J \cdot kg^{-1} \cdot K^{-1}$)
E	single cell open circuit voltage (V)
F	Faraday number (96485 C)
f	output free response
G	controller dynamic matrix
g_i	dynamic matrix coefficients
I	stack current (A)
i	current density ($A\ cm^{-2}$)
J	cost function
M_{O2}	oxygen molar mass (32×10^{-3} $kg\ mol^{-1}$)
m	control horizon
n	number of cells in the stack
P	power (W)

p	prediction horizon
p_{O2},p_{H2}	oxygen and hydrogen partial pressure (Pa)
Q, R	weight matrixes
T	temperature (K)
t	time (s)
u	control variable
U	future control vector
V	voltage (V)
W	flow rate (kg s^{-1})
w	output setpoint
$\hat{y}$	predicted output

Subscripts and superscripts

atm	atmospheric
aux	auxiliary
CM	compressor motor
CP	compressor
i, j	index
FC	fuel cell
rct	reacted
sys	system
T	transposed

Greek letters

γ	ratio of the specific heats of air (1.4)
ΔH	higher heating value of hydrogen (286 kJ)
η	efficiency
λ_{O2}	oxygen excess ratio

References

[1] S. Yerramalla, A. Davari, A. Feliachi, T, Biswas, J. of Power Sources, 124 (2003) pp. 104-113.

[2] J. Pukrushpan, H. Peng, A. Stefanopoulou, J. of Dynamics Systems, Measurement, and Control. 126 (2004) 14-25.

[3] J. Larminie, A. Dicks, Fuel Cell systems explained, Wiley, New York, 2000, pp.

[4] D. Friedman, R. Moore, Electrochemical Society Proceedings, 27 (1998) pp. 407-423.

[5] M. Grujicic, K. Chittajallu, E. Law, J. Pukrushpan, J. of Power and Energy, 218 (2004) 487-499.

[6] A. Vahidi, A. Stefanopoulou, H. Peng, Proceedings of the American Control Conference, (2004) 834-839.

[7] J. Golbert, D. Lewin, J. of Power Sources, 135 (2004) 135-151.

[8] F. Barbir, PEM Fuel Cells: Theory and Practice, Elsevier, 2005, pp. 280-288.

[9] E. Camacho, C. Bordons, Model Predictive Control, Springer-Verlag, Londres, 1999, pp. 33-39.

[10] M Serra, A. Husar, D. Feroldi, J. Riera, J. of Power Sources, 158 (2006) 1317–1323

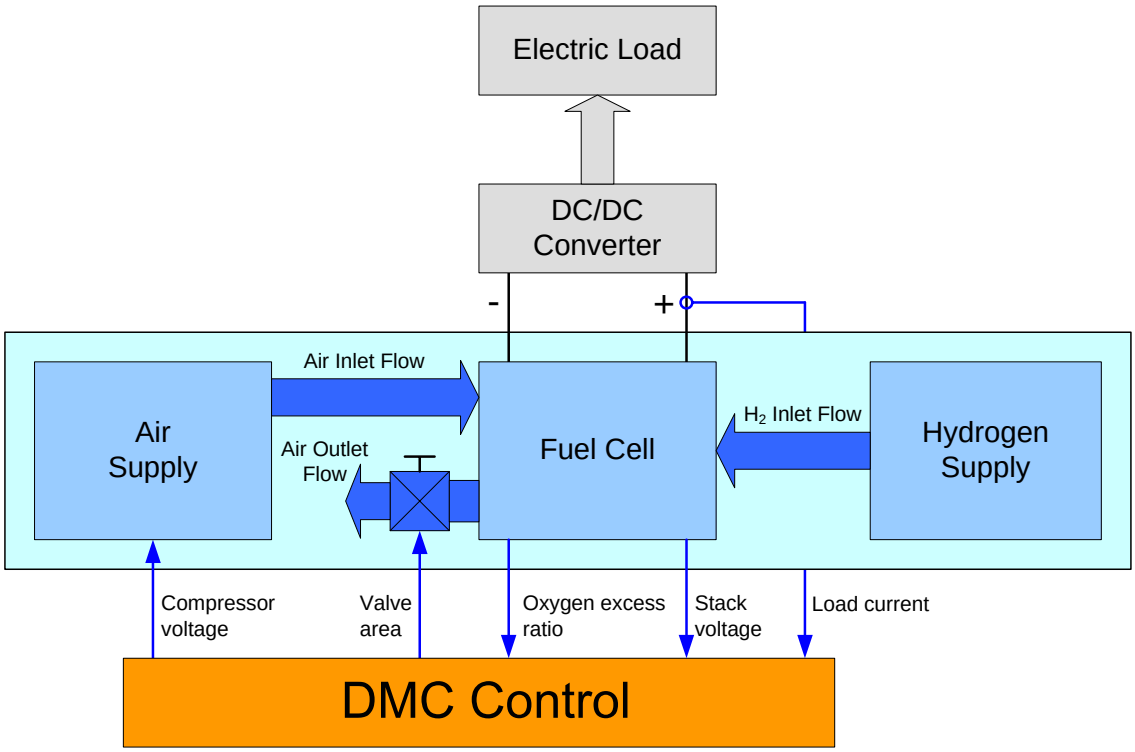

Fig. 1. PEM fuel cell system

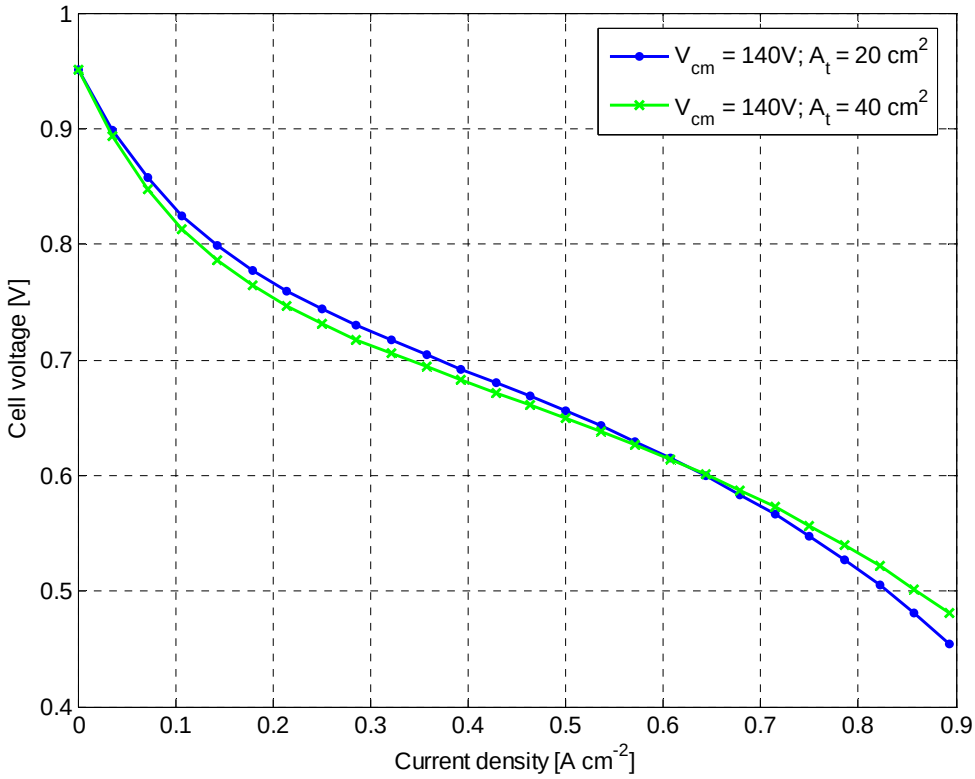

Fig. 2. Polarization curves with V_{cm} = 140V and different valve area

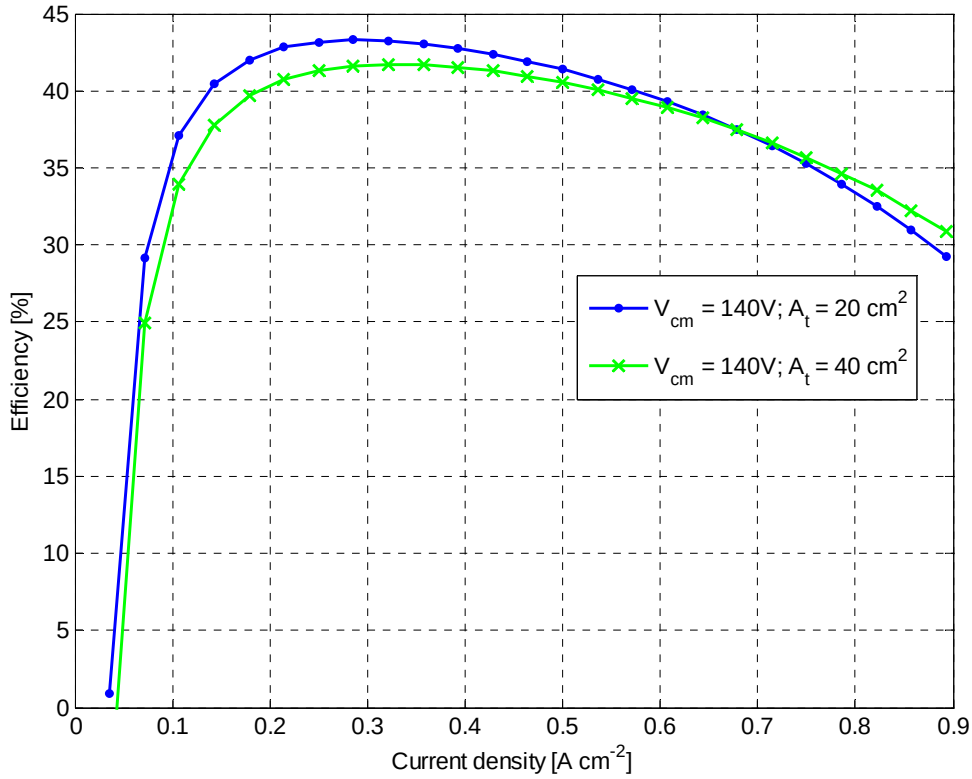

Fig. 3. Efficiency curves with V_{cm} = 140V and different valve area

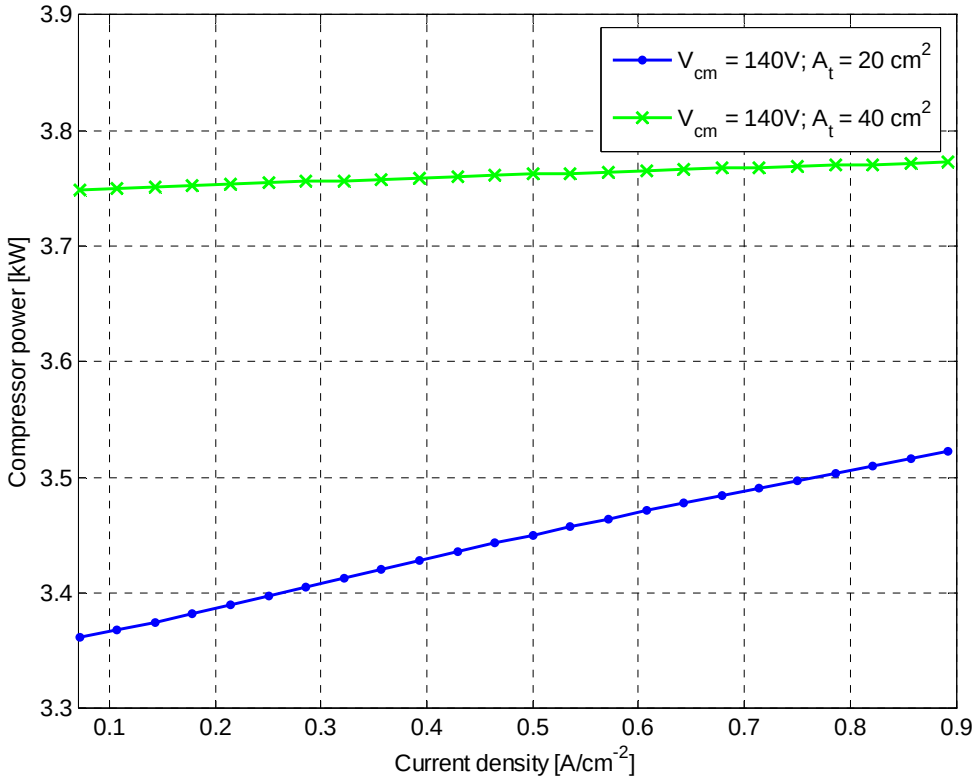

Fig. 4. Compressor power consumption curves with V_{cm} = 140V and different valve area

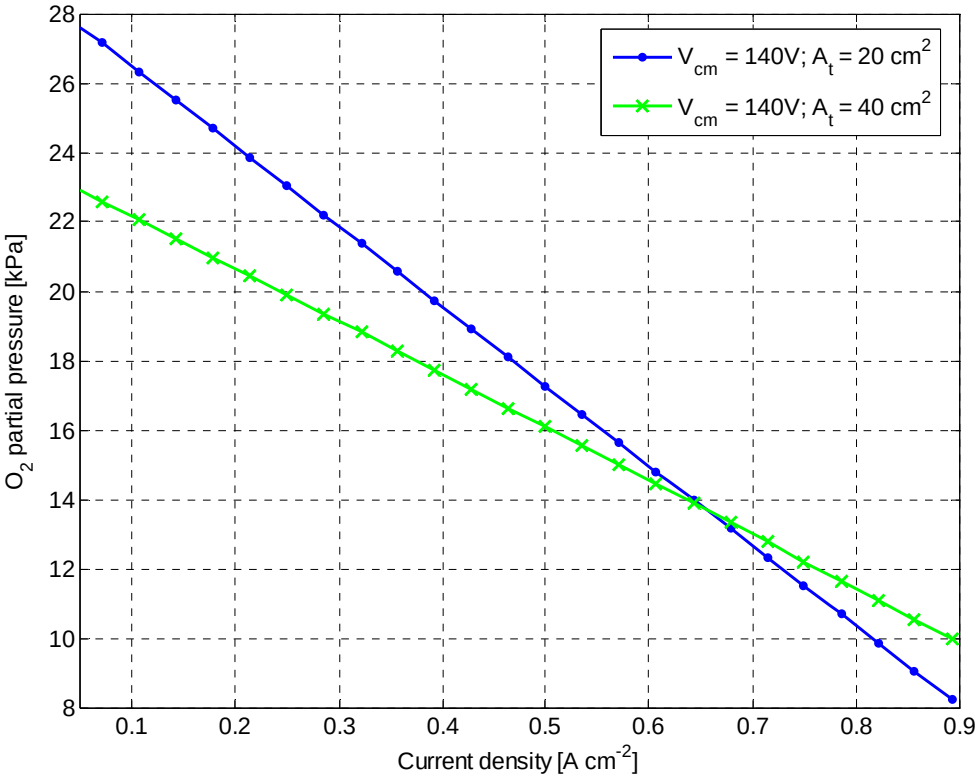

Fig. 5. Oxygen partial pressure curves with V_{cm} = 140V and different valve area

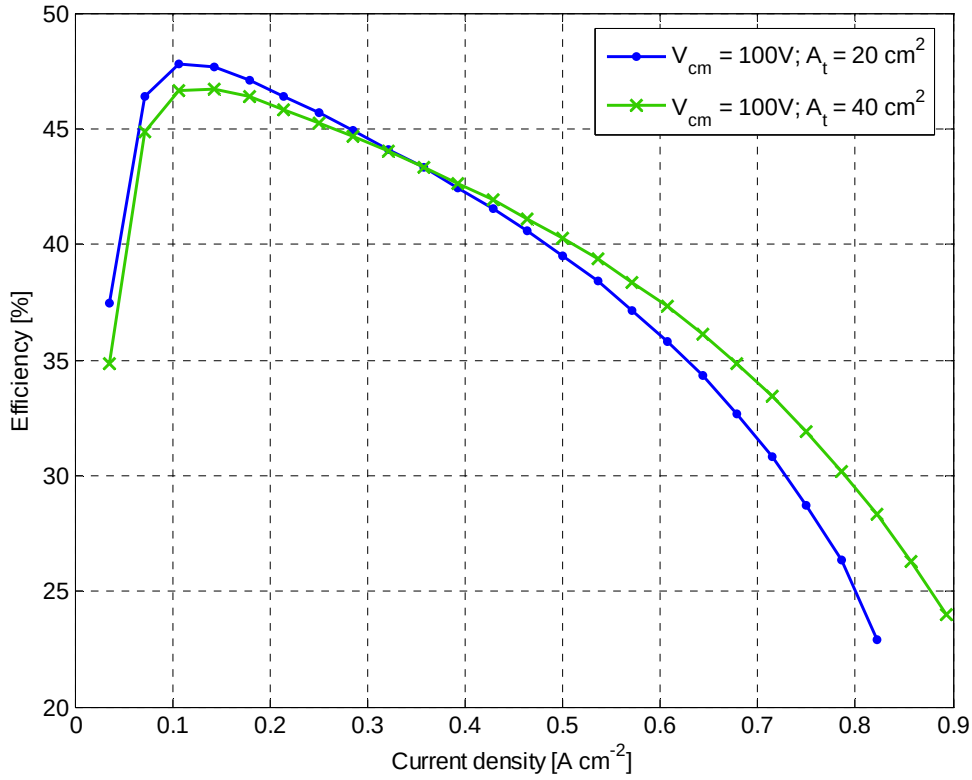

Fig. 6. Efficiency curves with V_{cm} =100V and different valve area

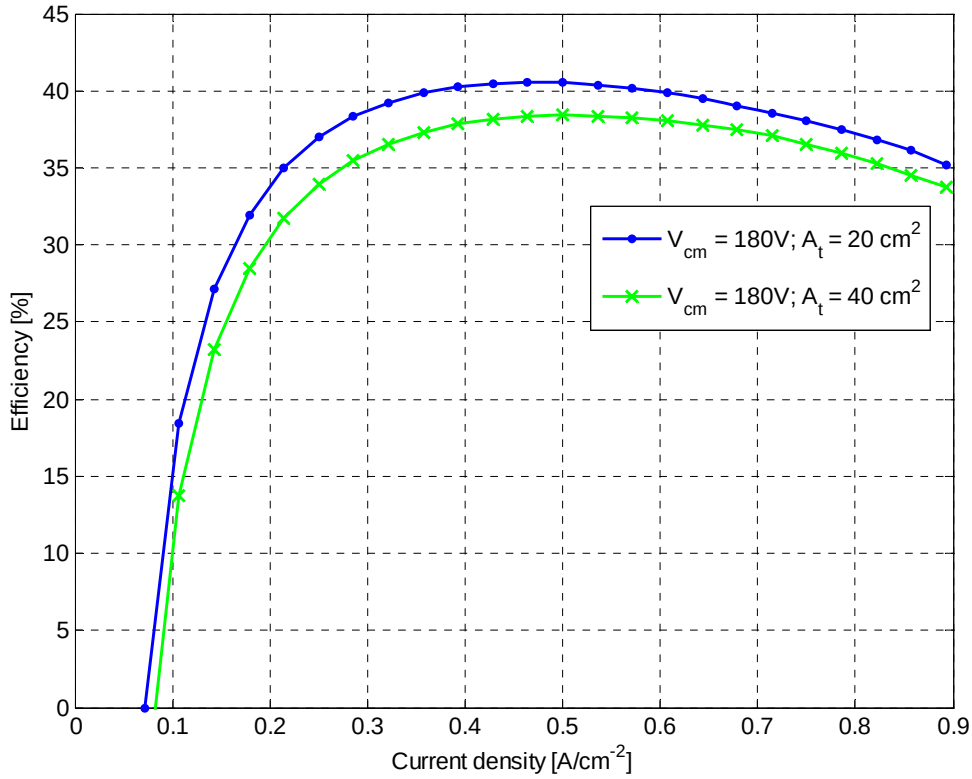

Fig. 7. Efficiency curves with V_{cm} =180V and different valve area

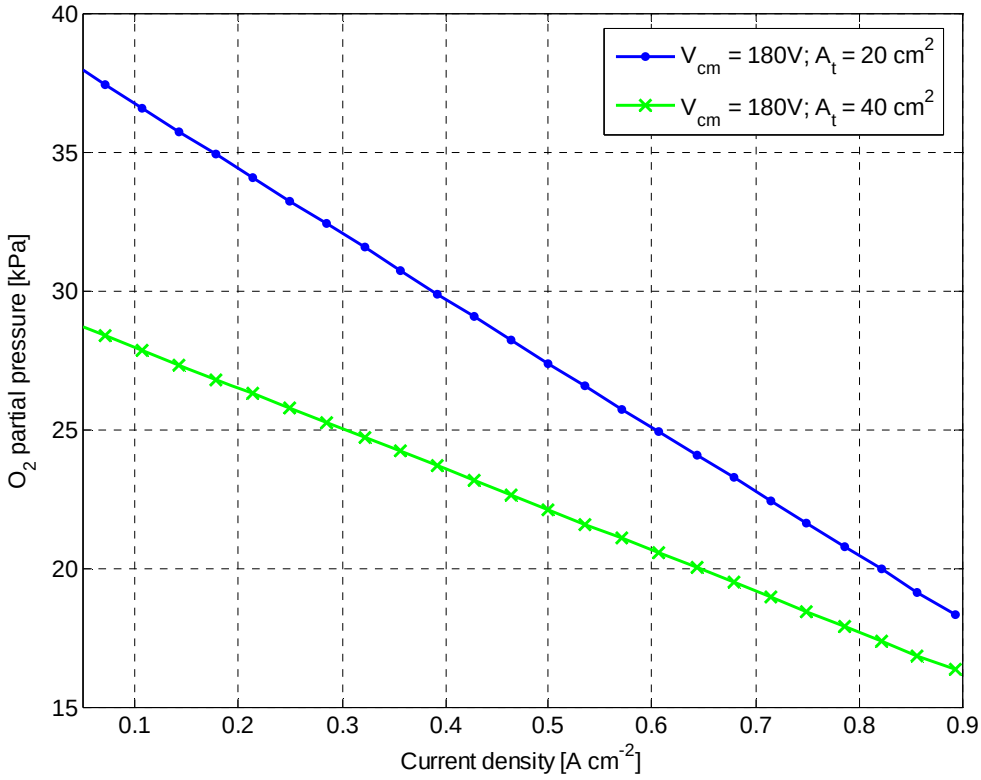

Fig. 8. Oxygen partial pressure curves with V_{cm} =180V and different valve area

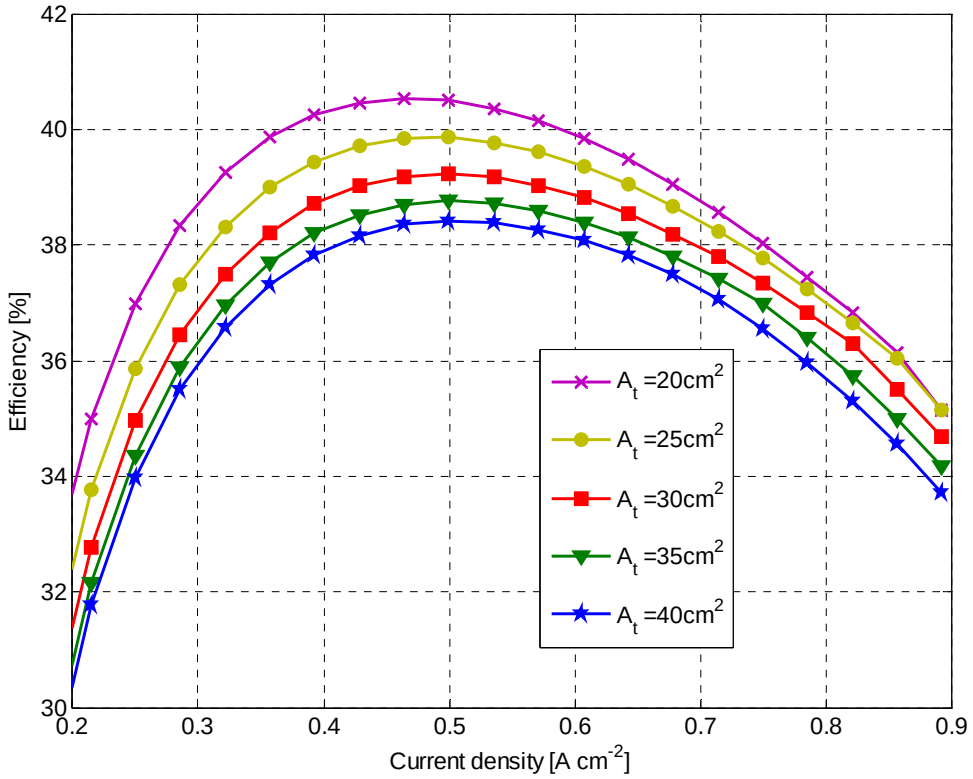

Fig. 9. Efficiency curves with V_{cm} =180V and different valve area

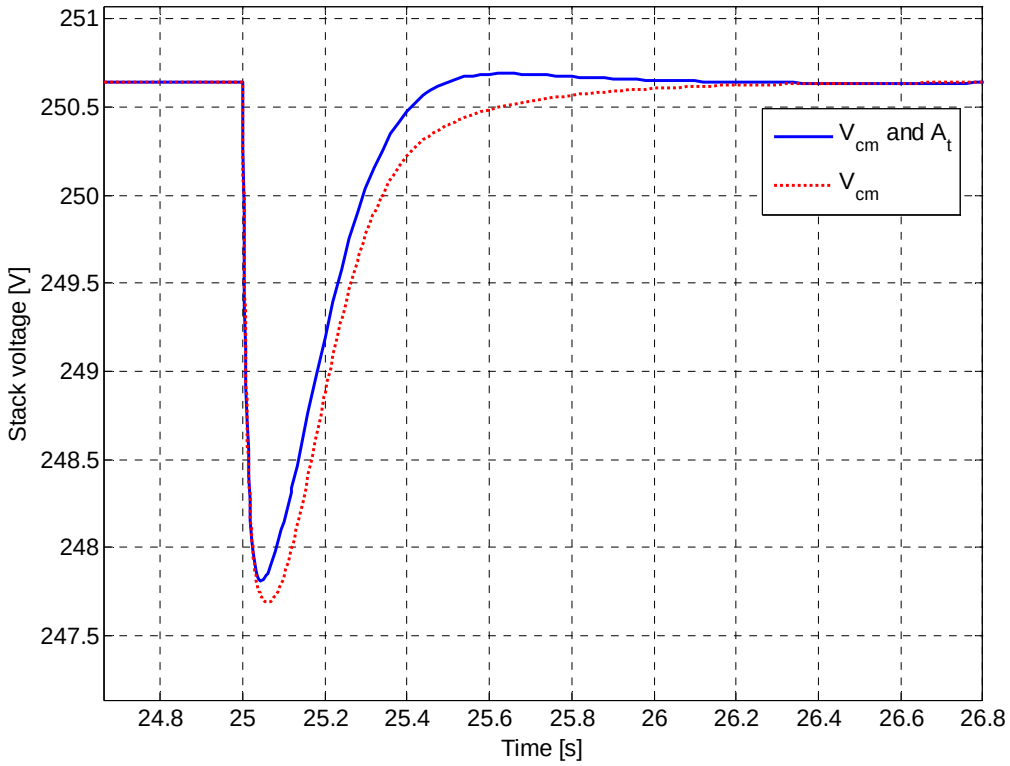

Fig. 10. Comparative between stack voltage responses

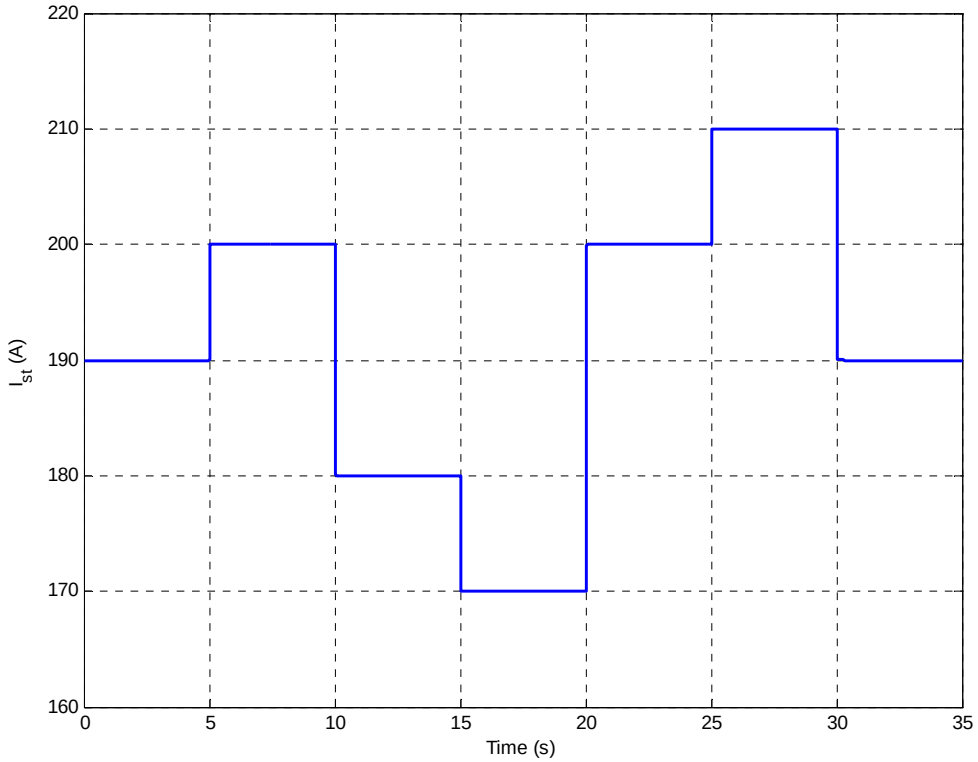

Fig. 11. Fuel cell stack current

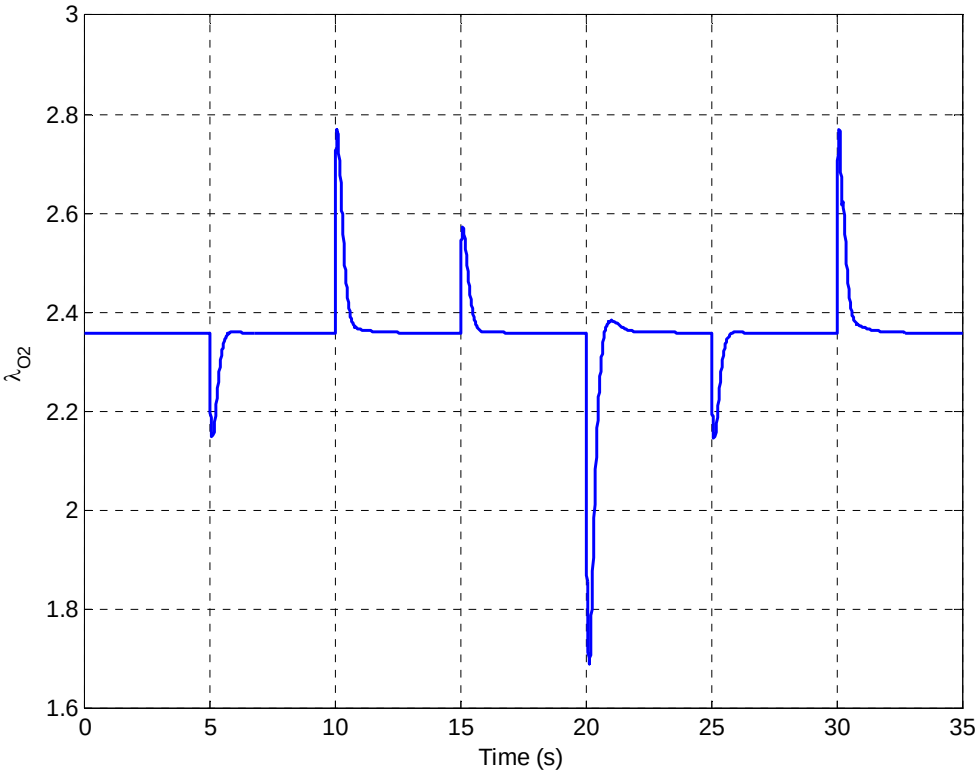

Fig. 12. Oxygen excess ratio

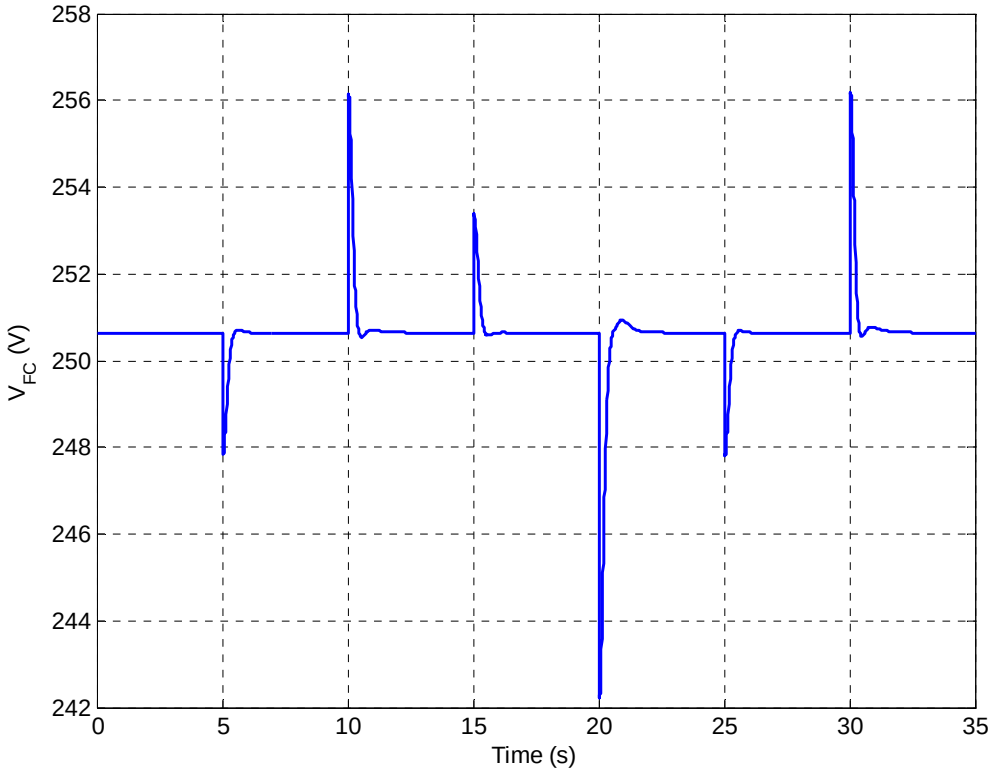

Fig. 13. Fuel cell stack voltage

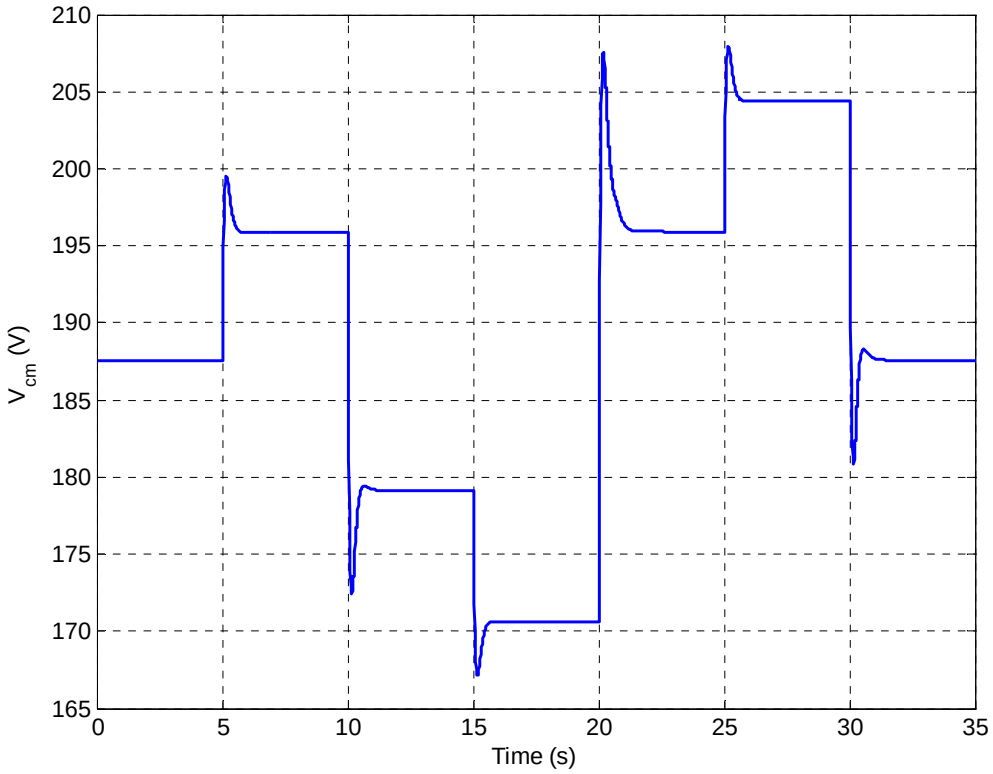

Fig. 14. Compressor motor voltage

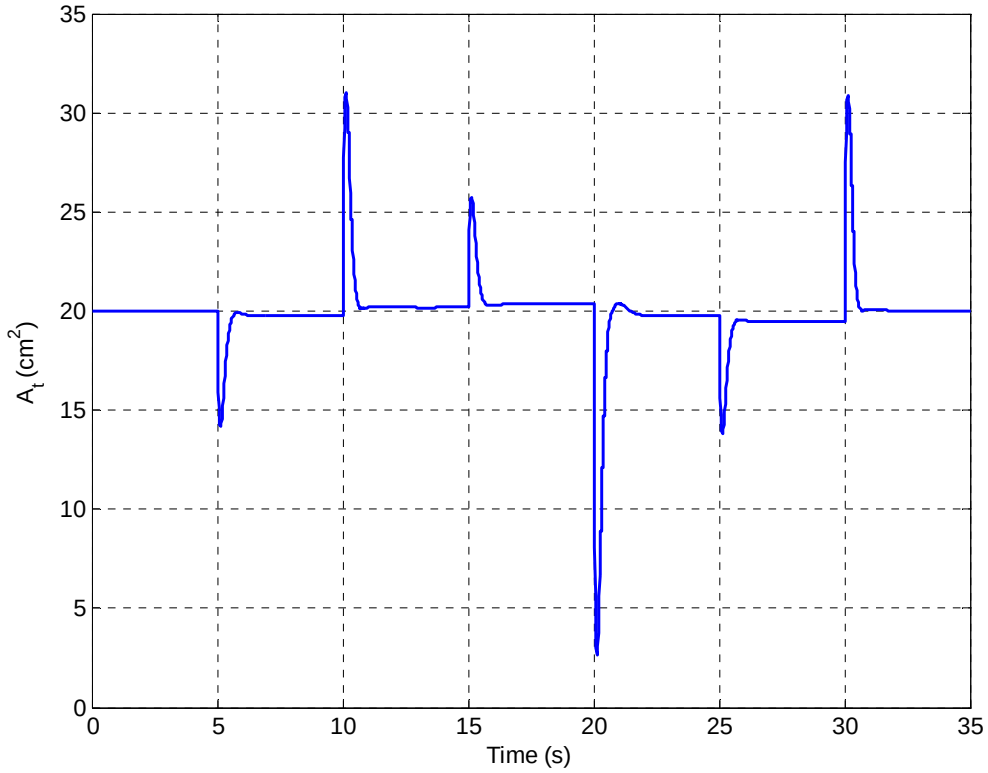

Fig. 15. Cathode air flow opening valve area

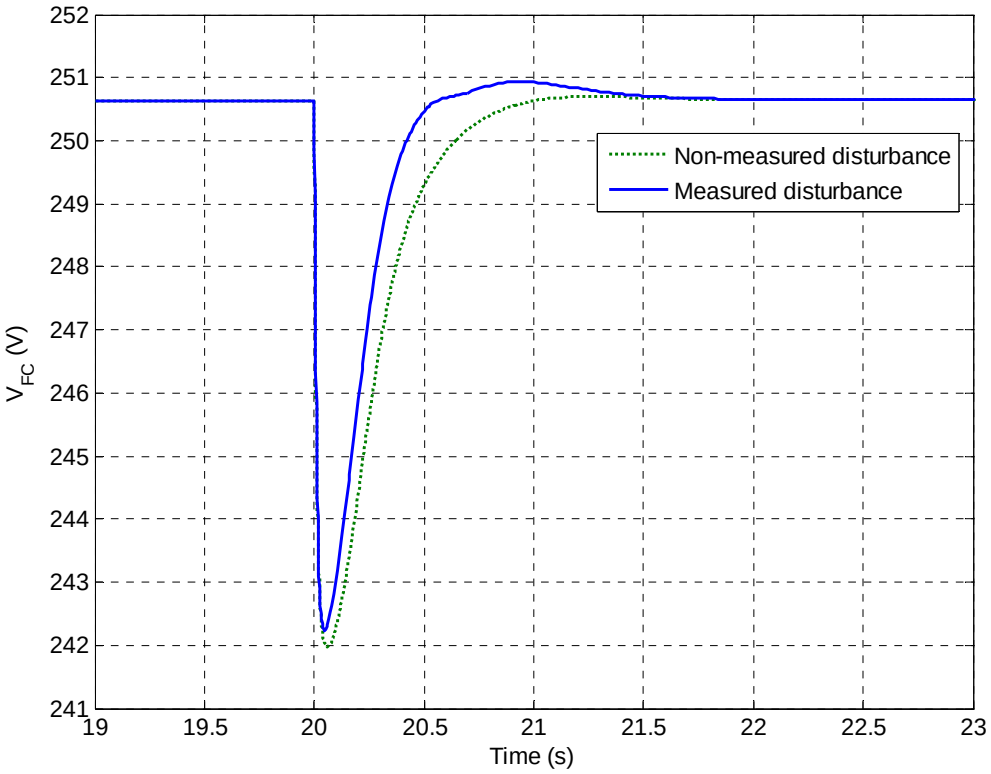

Fig. 16. Comparative between stack voltage response with measured and non measured disturbance

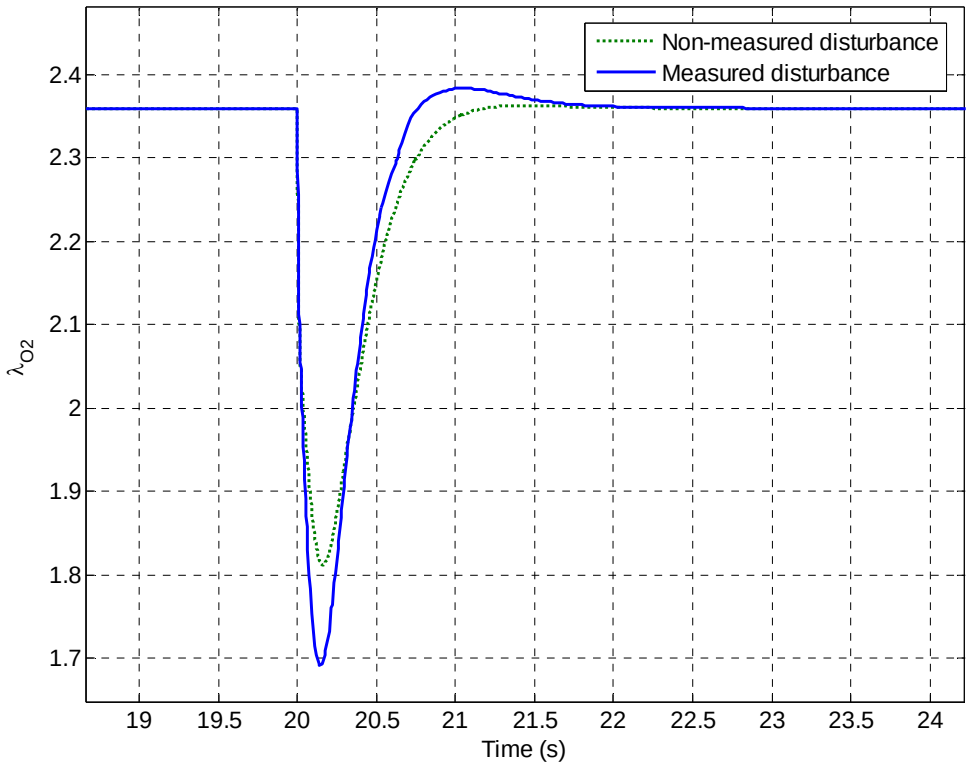

Fig. 17. Comparative between oxygen excess ratio response with measured and non measured disturbance